MedCrave
Step into the World of Research
Journal of Applied Biotechnology and Bioengineering

Review Article
Open Access
CrossMark

Aggregation of hydrophobic proteins: size dependent behavior and crossover to instability

Abstract

In this study, the aggregation properties of mainly hydrophobic proteins are explored by using an extended DLVO model that included an extra short-range interaction. Two different interaction regimes are studied to isolate the effect of hydrophobic interactions on protein aggregation. In the first interaction regime, van der Waals attraction, electrostatic double-layer repulsion, and short-range surface interactions are considered, and the interaction curves are described by finite energy barriers that kinetically stabilize protein dispersions over a broad size (R = 5-100 nm) and hydrophobicity (h_f = 0-20 %) range. In the second interaction regime, hydrophobic attraction is described by an exponential potential, causing the electrostatic barrier to collapse beyond a critical size, and resulting in a diffusion-limited, irreversible protein aggregation. The maximum interaction force (F_{max}) - size scaling analysis shows, $F_{max} \sim R^{\pm\alpha}$, with $\alpha = 0.5$ for the first interaction regime, whereas in the second (hydrophobicity-dominated) interaction regime, this scaling linearly decreases with size ($\alpha = -0.5$), indicating the lack of finite energy barriers and the dominance of short-range attraction. These results demonstrate that hydrophobic interactions by themselves are capable of inducing aggregation in electrostatically balanced systems. As a test, aggregation pattern in two predominantly hydrophobic proteins, elastin and zein, are discussed within the framework of Model-2 with satisfactory outcomes. Overall, this study clearly shows a size-dependent crossover from attraction-dominated behavior at small sizes to an unstable interaction regime at larger sizes, a conclusion that can be extended to colloidal, intrinsically disordered proteins and nanoparticle systems where surface hydrophobicity is profound.

Graphical abstract

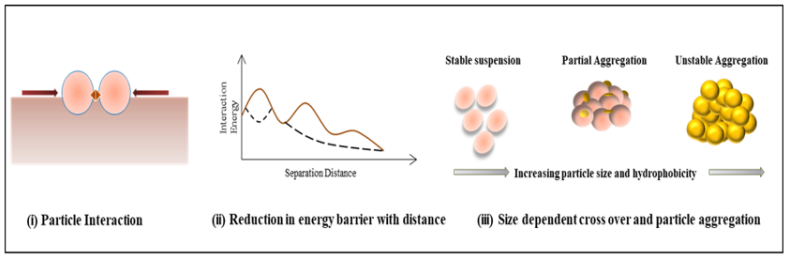

Interaction mechanisms in predominantly hydrophobic proteins lead to size dependent cross-over to instability due to increased hydrophobicity.

Keywords: hydrophobic protein aggregation, non-DLVO model, interaction potential, size-dependent crossover, interaction force-particle size scaling

Volume 13 Issue 3 - 2026

Neha VK, Himadri B Bohidar
Department of Applied Physics, Delhi Technological University, India

Correspondence: Himadri B Bohidar, Department of Applied Physics, Delhi Technological University Bawana Road, Delhi-110042, India

Received: June 30, 2026 | **Published:** July 16, 2026

Highlights: Hydrophobic proteins undergo distinctive aggregation unlike normal proteins.

Hydrophobic and surface forces must be included in the DLVO theory to address this issue.

The extended DLVO formulation revealed scaling of maximum interaction force with size.

Under dominating hydrophobic interactions, a size and hydrophobicity dependent crossover to instability was noticed.

Introduction

Self-assembly or aggregation of proteins is the most significant contributor to neurological and neurodegenerative pathogenic conditions like, the Alzheimer's, Parkinson's, Huntington, Amyotrophic Lateral Sclerosis, Creutzfeldt Jakob Dementia, Prion diseases, Amyloidosis and other forms of dementia. Proteinopathy is a recently coined term which refers to the conditions where proteins become structurally abnormal or fail to fold into stable secondary structures. This morphological change may contribute to the formation of oligomeric aggregates that adversely interfere with multiple biochemical processes leading to serious pathological consequences. Therefore, it is pertinent to develop a better understanding of this phenomenon.

Proteins are biopolymers composed of polar and non-polar amino acids arranged along a peptide backbone.[1] When dispersed in aqueous environment, the exposure of hydrophobic amino acid residues to water is energetically unfavourable that leads to their partial exclusion from the protein surface and the emergence of cooperative folding forces that organize the protein interior.[2] As a result, hydrophobic residues tend to cluster, forming compact structural motifs that stabilize native conformations while simultaneously influencing long-range intermolecular interactions. This hydrophobic driving force plays a central role in protein self-assembly, misfolding, and aggregation phenomena.[2,3] There exist a class of proteins that are structurally disordered (intrinsically disordered proteins, IDPs), and

proteins comprising of large amount of hydrophobic amino acids (like leucine, isoleucine, valine, phenylalanine, and methionine) that exhibit aggregation behaviour not accountable by DLVO type description.[4] Some examples of IDPs are p27, p53, CREB α-synuclein, tau, elastin, CREB, amyloidogenic proteins etc. These proteins are characterised by their short-range folding complexity and unusual aggregation tendency. Among the hydrophobic proteins elastin, zein, prolamin, silk fibroin and transmembrane proteins are biologically relevant.[5,6] Therefore, understanding the interaction mechanisms that lead to the aggregation pattern of these predominantly hydrophobic biomolecules is necessary, furthermore such a model must account for the degree of hydrophobicity, and size of the biomolecules among other parameters.

From a physical standpoint, proteins in solution may be viewed as complex colloidal particles whose stability is governed by the balance between attractive and repulsive intermolecular forces.[7] The classical Derjaguin-Landau-Verwey-Overbeek (DLVO) theory is a fundamental theoretical basis for understanding such interactions, taking into consideration the competition between the van der Waals attraction and the electrostatic repulsive forces due to the overlap of the electric double layers.[8] The interaction potential usually has a strong primary minimum at short range, a finite repulsive energy barrier at intermediate range, and a shallow secondary minimum at long range.[9] Aggregation takes place when the attractive forces prevail or when the electrostatic barrier is sufficiently lowered, allowing access to the primary minimum.[10] Salt-mediated aggregation of colloids and proteins is a result of DLVO-type interactions.[8,11–13]

A stable dispersion of biomolecules in water requires its proper hydration by the creation of successive hydration layers around its surface.[14] In the case of biomolecules with high hydrophobicity, such hydration becomes problematic, and therefore the stability of their dispersion must be considered properly by taking into consideration their hydrophobicity.[15] Hydrophobic proteins, in particular, owing to their special amino acid composition, are problematic in terms of traversing their free-energy landscape of dispersion stability in water.[16]

In this prominent biopolymer category, the presence of non-polar side chains promotes hydrophobic interactions and affects the interfacial water structure, thus deviating from the predicted balance according to classical DLVO theory.[3] In aqueous solution, hydrogen bonding between biomolecular functional groups and water molecules is a fundamental mechanism in the stabilization of biomolecular structures, whereas hydration layers and solvent structuring effects introduce new short-range forces that are not accounted for in the classical DLVO theory.[17] At the molecular level, binding attraction forces can be modelled using Lennard-Jones or Morse potentials, which are versatile models of short-range binding forces in biomolecular association.[18]

Therefore, a complete understanding of hydrophobic protein aggregation must necessarily incorporate the interaction model with non-DLVO contributions such as hydrophobic forces and surface-specific forces.[8] These extended DLVO models, based on colloid and polymer physics, provide a physically consistent framework for understanding the potential impact of hydrophobic regions on interaction forces and the aggregation of proteins into larger, typically biologically inactive entities.[2,3,8]

Modified DLVO theory

Though the traditional DLVO theory is able to capture the balance between the attraction and electrostatic repulsion forces, it does not take into account the molecular hydrophobicity. Moreover, the biomolecular surface interaction often involves other forces, such as interfacial, steric, depletion, solvation forces, etc., which were not taken into account in the traditional DLVO theory.[19] Hydrophobic association, hydration, steric repulsion, and surface organization have been found to play a substantial role in protein systems, especially when non-polar amino acid regions are predominant in intermolecular interactions[3]. Consequently, the total interaction potential is represented by an extended form in which extra surface potentials or short-range exponential terms are incorporated along with the classical van der Waals and double-layer contributions.[20,21]

The constitutive interaction potential is therefore written as a sum of: (i) dispersion or molecular-scale attraction, (ii) electrostatic repulsion, (iii) and an additional term representing surface or hydrophobic interactions given by

$$U_{total} = [U_{attr} + U_{rep}]_{DLVO} + [U_{add}]_{non-DLVO} \quad (1)$$

Here, U_{attr} may take Lennard–Jones (van der Waals) interaction term, or plate-plate or hydrophobic exponential form, U_{rep} represents the electric-double-layer (Debye-Hückel type) term derived from linearized Poisson-Boltzmann theory and, U_{surf} accounts for hydration, steric or surface contributions. Typically, the first-two potentials on the right comprise the DLVO interactions while the additional potential U_{add} is introduced to account for other interactions mentioned earlier.

Molecular hydrophobicity, in particular, may significantly deepen the primary minimum even under stabilizing electrostatic conditions, thereby offering a physical route toward the aggregation of hydrophobic proteins.[22] Clearly, a realistic model to describe the protein stability must encompass its degree of hydrophobicity as well as its physical size which is the main objective of this work. Herein, the consequences of these additional interactions are examined through systematic model calculations to highlight their bearing on the protein stability.

Mathematical modelling

In order to evaluate the combined influence of attractive, electrostatic and surface-specific forces, numerical interaction profiles were generated by superposing three potential components. The calculations are based on dimensionless coordinates r/R and $U(r)/k_BT$, where R denotes an effective particle size and k_BT is the thermal energy at temperature T and U(r) is the interparticle interaction potential. This representation permits comparison across different sizes and surface fractions without altering the underlying functional forms.[3,23]

(a) Model – 1

The first model employs a Lennard-Jones term for short-range molecular attraction $\mathbf{U_{LJ}}$, together with the Debye-Hückel electrostatic double-layer potential $\mathbf{U_{DL}}$ and a surface exponential term $\mathbf{U_{surf}}$ describing hydrophobic or hydration forces given by

$$U_{total} = U_{LJ} + U_{DL} + U_{surf} \quad (2)$$

Lennard–Jones potential U_{LJ} captures hard-core exclusion at very short separations followed by an attractive tail consistent with molecular pair interactions[24] given by

$$U_{LJ}(r) = 4\varepsilon\left[\left(\frac{\sigma}{r+\sigma_0}\right)^{12} - \left(\frac{\sigma}{r+\sigma_0}\right)^{6}\right] \quad (3)$$

Citation: Neha VK, Bohidar HB. Aggregation of hydrophobic proteins: size dependent behavior and crossover to instability. *J Appl Biotechnol Bioeng* . 2026;13(3):91–98. DOI: 10.15406/jabb.2026.13.00422

σ is the molecular length and ε defines the strength of the potential. σ_0 is the small shift to avoid singularity at $r=0$. This potential comprises of a very short-range repulsion $(\propto r^{-12})$ plus long-range attraction $(\propto r^{-6})$.

Double Layer interaction is a repulsive interaction decaying with a screening length κ^{-1} (Debye length) is given by[25]

$$U_{DL}(r) = A_{DL}\frac{a}{a+r}e^{-kr} \qquad (4)$$

A_{DL} is a constant set by surface potential/ionic strength.

The additional potential term U_{add} is taken as a phenomenol λ_{surf} term parameterised by the magnitude C_{surf} and decay length representing hydrophobic attraction structuring is given by

$$U_{surf}(r) = C_{surf}\, ae^{-r/\lambda_{surf}} \qquad (5)$$

(b) Model – 2

The second model replaces the Lennard-Jones attraction with a tunable hydrophobic exponential potential (Eq. 6), thereby isolating the effect of hydrophobic forces without invoking a strong hard-core repulsion. This potential is given by

$$U_{hydro}(r) = -A_h\frac{a}{a+r}e^{-r/\lambda_h} \quad (6)$$

Where A_h controls the amplitude and λ_h sets the range of this potential.[15] This potential is characterized by a short-range interaction (attraction) with sufficient tunability to produce deeper primary minimum without adding hard-core repulsion. The two models are logically constructed to distinguish kinetically stabilized interaction landscapes to smoothly navigate from the hydrophobicity-dominated aggregation regimes. This way of formulation enables the depth of the primary well to be varied independently by changing the hydrophobic amplitude and range. In this case, aggregation can be initiated without necessarily lowering the electrostatic barrier, as seen in hydrophobic protein systems.[26] Figure 1 captures the essential features of the two models discussed. Their relevance will be further established in the discussions that follows.

Choice of model parameters

To facilitate a controlled comparison between the two interaction models, all calculations were conducted with the same set of numerical bias and interaction parameters, and the variations were introduced only as explicitly stated. In the structured analysis, a hydrophobic surface fraction of $h_f = 10\%$ (degree of hydrophobicity) was chosen as the basis for further analysis. This is a weak to moderate level of hydrophobicity which is sufficient to impact near-contact interactions but with a finite electrostatic energy barrier. The same hydrophobic fraction was used for both models, such that any differences in interaction behavior are due solely to the contribution of the attractive interaction.

Baseline interaction parameters

In Model-1, the short-range attraction was modelled using a Lennard-Jones potential. The energy scale was set at $\varepsilon = 20\,k_BT$ and the molecular length scale $\sigma = 0.35\,nm$. To avoid divergence when particles get too close, a small shift parameter $r_0 = 0.05\,nm$ was introduced which make certain about the numerical stability at contact. For the electrostatic repulsion, both models used the Debye-Huckel form. The prefactor was $A_{DH}=30\,k_BT$ and a Debye length of $\lambda_D = \kappa^{-1} = 0.8\,nm$. These values were kept fixed in all simulations to maintain identical electrostatic bias. A short-range surface interaction was included with an amplitude $C_{surf} = 3\,k_BT\,nm^{-1}$ and a decay length $\lambda_{surf} = 6\,nm$. This part accounts for extra effects near the surface and was adjusted based on the hydrophobic surface fraction h_f when needed.

Hydrophobic interaction parameters

Model-2 was designed with hydrophobic attraction which was explicitly added by an exponential interaction characterized by a strength $A_h = 80\,k_BT$ and a decay length $\lambda_h = 0.35\,nm$. These parameters were chosen to model strong and short-range hydrophobic interactions relevant to biomolecular and colloidal systems, while permitting direct comparison with the Lennard-Jones attraction used in Model-1.

Particle Size and hydrophobicity dependence

Baseline interaction profiles and stability were studied at a fixed particle size of $a = 5nm$ under the same bias conditions described earlier. Particle separation was expressed using the dimensionless distance r/R, where R denotes the effective particle size.

To examine the influence of hydrophobicity on interaction potentials and stability, the hydrophobic surface fraction was varied systematically across h_f = 0%, 5%, 10%, 15%, and 20%. This analysis was performed for both the models at particle sizes R = 5, 25, 50, 75, and 100 nm, enabling a combined assessment of surface and particle size effects. Interaction regimes were classified according to the magnitude of the energy barrier separating attractive and repulsive regions: (i) stable regime ($U_{bar} > 10\,k_BT$), (ii) metastable regime ($1 < U_{bar} \leq 10\,k_BT$), and (iii) unstable regime ($U_{bar} \leq 1\,k_BT$). This classification provides a consistent framework in comparing kinetic stability for various models and parameter sets. Furthermore, it will be appropriate to place the energy scales discussed above in the right perspective *vis a vis* protein aggregation. At the room temperature (300 K), the thermal energy k_BT is close to the hydrogen bond energy (i.e. few kcal/mol). Often the aggregation in biopolymers, and the proteins in particular, is due to the formation of intermolecular hydrogen bonds.[27] Thus, the energy requirement for the stability defined above (10 k_BT) is equivalent to saying any aggregate with at least ~10 H-bond contacts is rigid and stable. The intermolecular interactions play a key role in bringing individual molecules closer. Then, the secondary forces get activated and aggregation ensues. In the discussion that follows, the models predict the energy barrier that must be overcome to establish aggregation.

All interaction energies were normalized by the thermal energy scale k_BT, and results are presented using the reduced interaction potential U/k_BT and the dimensionless separation r/R. Interaction forces were obtained from the first derivative of the interaction potential with respect to separation. The maximum attractive force was extracted for each particle size, and a linear fitting was performed between the maximum interaction force F_{max} and particle size R to quantify size-dependent force scaling under fixed hydrophobic and electrostatic conditions.

Results

The two interaction models yield qualitatively different short-range interaction landscapes at 10% hydrophobicity and particle size R=5 nm. A stable interaction profile with a finite primary minimum separated from contact by an energy barrier was noticed in Model-1. This can be interpreted as the combined effects of Lennard–Jones attraction, electrostatic repulsion, and surface interactions. In contrast,

Model-2 exhibits a strongly attractive short range interaction dominated by a hydrophobic exponential potential (Figure 1). Although an electrostatic contribution is present, the overall interaction profile doesn't display a pronounced stabilizing barrier separating the primary minimum from particle contact. The depth of the attractive well in Model-2 is substantially greater than that of model-1 under identical biases. The detailed contributions of the each interaction terms and the resulting potential profiles can be observed in Figures 2 & 3.

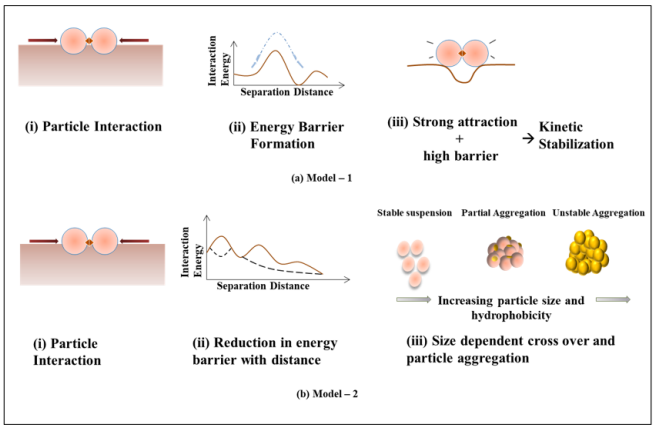

Figure 1 Interaction landscapes for the two interaction models. (a) Model-1 has a deep primary minimum separated by a finite energy barrier due to a balance of short-range Lennard-Jones attraction and electrostatic repulsion, leading to kinetically stable dispersions. (b) Model-2 illustrates the aggregation phenomenon caused by hydrophobicity, where increasing particle size and hydrophobicity continue to decrease the energy barrier until it collapses, leading to a transition from a stable dispersion to an aggregation state.

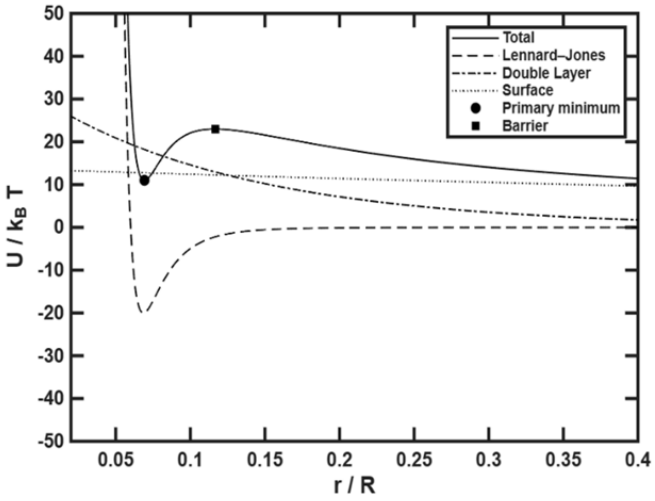

Figure 2 Model-1 interaction potential for 10% hydrophobicity at R=5 nm, showing Lennard–Jones attraction, electric double-layer repulsion and surface contributions with a clearly resolved primary minimum and barrier.

Effect of hydrophobicity

The dependence of the interparticle interaction potential on hydrophobicity in Model-1 for a particle size of 50 nm is presented in Figure 4, and the results for particle sizes of 25, 75, and 100 nm are presented in Figure S1 (Supporting Information). For all particle sizes, the systematic increase in the hydrophobic surface fraction results in a systematic increase in the depth of the primary minimum of the interaction potential. The location of the primary minimum is independent of the hydrophobic fraction, with the equilibrium location at $r_{min} \approx 0.34$ nm.

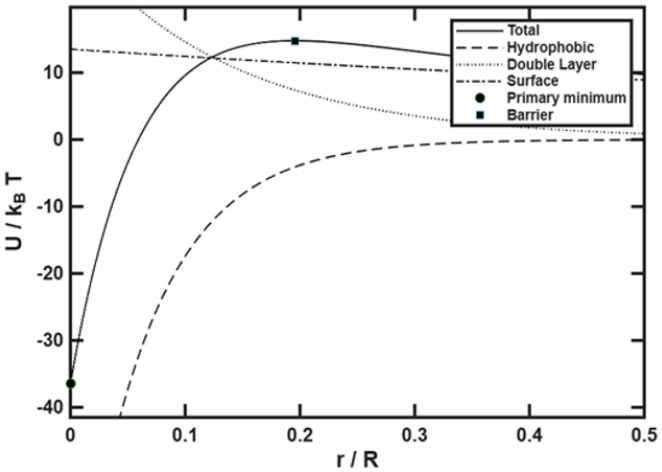

Figure 3 Model-2 interaction potential for 10% hydrophobicity at R=5 nm, demonstrating a deep hydrophobic well and a finite electrostatic barrier in the short-range molecular regime.

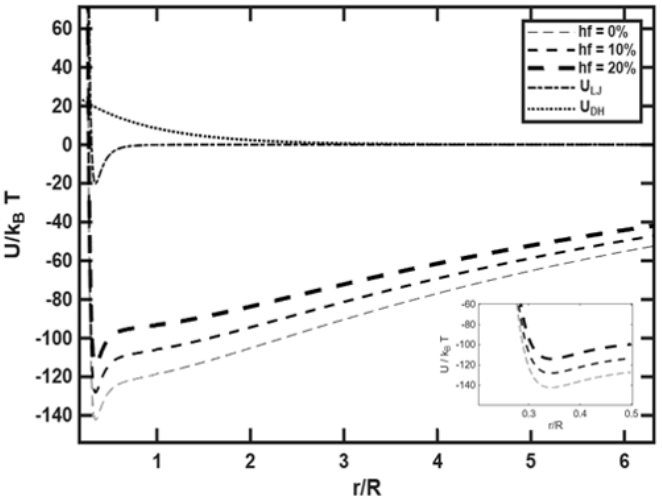

Figure 4 Hydrophobicity dependence of the interparticle interaction potential in Model-1 for particle size R=50 nm.

The region near contact shows the existence of a finite energy barrier between the primary minimum and larger separations for smaller particle sizes. At $R = 25\ nm$, a pronounced barrier is observed for all hydrophobic fractions, whereas for particle sizes of *50 nm* and above the barrier height progressively decreases and eventually vanishes. The corresponding quantitative values of the interaction minimum U_{min}, equilibrium separation $r_{min,}$ barrier height U_{bar}, and stability regimes are summarized in Tables 1–4 (Supporting Information).

Table 1 Hydrophobicity dependence of interaction minimum, barrier height, and stability regime for Model-1 at R = 25 nm

h_f (%)	U_{min}/k_BT	r_{min}(nm)	U_{bar}/k_BT	Regime
0	-71.51	0.34	16.18	Stable
5	-67.97	0.34	15.94	Stable
10	-64.43	0.34	15.72	Stable
15	-60.89	0.34	15.51	Stable
20	-57.35	0.34	15.31	Stable

Citation: Neha VK, Bohidar HB. Aggregation of hydrophobic proteins: size dependent behavior and crossover to instability. *J Appl Biotechnol Bioeng* . 2026;13(3):91–98. DOI: 10.15406/jabb.2026.13.00422

Table 2 Hydrophobicity dependence of interaction minimum, barrier height, and stability regime for Model-1 at R = 50 nm

h_f (%)	U_{min}/k_BT	r/R	U_{bar}/k_BT	Regime
0	-142.20	0.34	0.00	Unstable
5	-135.12	0.34	0.00	Unstable
10	-128.04	0.34	0.00	Unstable
15	-120.96	0.34	0.00	Unstable
20	-113.87	0.34	0.00	Unstable

Table 3 Hydrophobicity dependence of interaction minimum, barrier height, and stability regime for Model-1 at R = 75 nm

h_f (%)	U_{min}/k_BT	r/R	U_{bar}/k_BT	Regime
0	-213.00	0.34	0.00	Unstable
5	-202.37	0.34	0.00	Unstable
10	-191.74	0.34	0.00	Unstable
15	-181.12	0.34	0.00	Unstable
20	-170.49	0.34	0.00	Unstable

Table 4 Hydrophobicity dependence of interaction minimum, barrier height, and stability regime for Model-1 at R = 100 nm

h_f (%)	U_{min}/k_BT	r/R	U_{bar}/k_BT	Regime
0	-282.83	0.34	0.00	Unstable
5	-269.66	0.34	0.00	Unstable
10	-255.48	0.34	0.00	Unstable
15	-241.31	0.34	0.00	Unstable
20	-227.14	0.34	0.00	Unstable

Figure 5 presents the hydrophobicity dependence of the interparticle interaction potential in Model-2 for a particle size of 50 nm; the corresponding results for the remaining particle sizes are included in the Supporting Information (Figure S2). For all particle sizes, the total interaction potential remains monotonic in nature without the formation of a primary minimum. Increasing the hydrophobic surface fraction produces a uniform downward shift of the interaction curves and reduces the magnitude of the interaction potential.

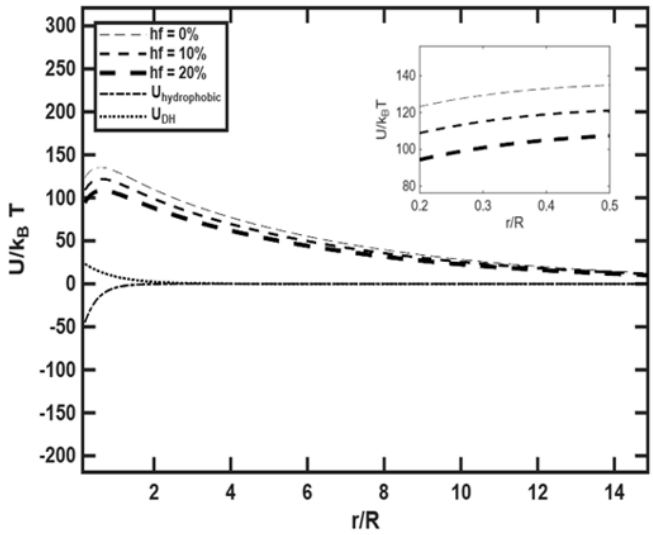

Figure 5 Hydrophobicity dependence of the interparticle interaction potential in Model-2 for particle size R=50 nm.

The near-contact region reveals that there is neither an energy barrier nor an equilibrium for any hydrophobic fraction and particle size. This behaviour is true for the entire range of particle sizes studied. The corresponding values of the interaction minimum $U_{min,}$ barrier height U_{bar}, and stability classification are listed in Tables 5–8 (Supporting Information).

Table 5 Hydrophobicity dependence of interaction minimum, barrier height, and stability regime for Model-2 at R = 25 nm

h_f (%)	U_{min}/k_BT	r/R	U_{bar}/k_BT	Regime
0	1.17	25.00	0.00	Unstable
5	1.12	25.00	0.00	Unstable
10	1.06	25.00	0.00	Unstable
15	1.00	25.00	0.00	Unstable
20	0.94	0.00	0.00	Unstable

Table 6 Hydrophobicity dependence of interaction minimum, barrier height, and stability regime for Model-2 at R = 50 nm

h_f (%)	U_{min}/k_BT	r/R	U_{bar}/k_BT	Regime
0	2.35	25.00	0.00	Unstable
5	2.23	25.00	0.00	Unstable
10	2.11	25.00	0.00	Unstable
15	2.00	25.00	0.00	Unstable
20	1.88	25.00	0.00	Unstable

Table 7 Hydrophobicity dependence of interaction minimum, barrier height, and stability regime for Model-2 at R = 75 nm

h_f (%)	U_{min}/k_BT	r/R	U_{bar}/k_BT	Regime
0	3.52	25.00	0.00	Unstable
5	3.35	25.00	0.00	Unstable
10	3.17	25.00	0.00	Unstable
15	2.99	25.00	0.00	Unstable
20	2.82	25.00	0.00	Unstable

Table 8 Hydrophobicity dependence of interaction minimum, barrier height, and stability regime for Model-2 at R = 100 nm

h_f (%)	U_{min}/k_BT	r/R	U_{bar}/k_BT	Regime
0	4.70	25.00	0.00	Unstable
5	4.46	25.00	0.00	Unstable
10	4.23	25.00	0.00	Unstable
15	3.99	25.00	0.00	Unstable
20	3.76	25.00	0.00	Unstable

Stability analysis

The stability regime classification for Models-1, 2 is shown in Figure 6. This classification is made on the basis of the height of the energy barrier that separates the attractive and repulsive interaction regions. In Model-1, the interaction regions are mostly in the stable regime for the entire range of particle sizes with finite barrier heights. The corresponding values of the primary minimum, energy barrier height, and maximum interaction force for a specific hydrophobic fraction are given in Table 9 (Supporting Information).

Table 9 Size-dependent interaction energies, forces, and stability regimes in Model-1 (h_f = 10%)

R (nm)	Primary min (k_BT)	Barrier (k_BT)	Stability Regime
5	-14.446	12.982	I
10	-26.581	13.656	I
15	-39.114	18.444	I
20	-51.752	24.146	I
25	-64.433	29.888	I

Citation: Neha VK, Bohidar HB. Aggregation of hydrophobic proteins: size dependent behavior and crossover to instability. *J Appl Biotechnol Bioeng* . 2026;13(3):91–98. DOI: 10.15406/jabb.2026.13.00422

30	-77.135	35.651	I
35	-89.851	41.426	I
40	-102.58	47.208	I
45	-115.3	52.995	I
50	-128.04	58.786	I
55	-140.78	64.58	I
60	-153.52	70.376	I
65	-166.26	76.174	I
70	179	81.974	I
75	-191.74	87.775	I
80	-204.49	93.577	I
85	-217.24	99.381	I
90	-229.99	105.18	I
95	-242.73	110.99	I
100	-255.48	116.8	I

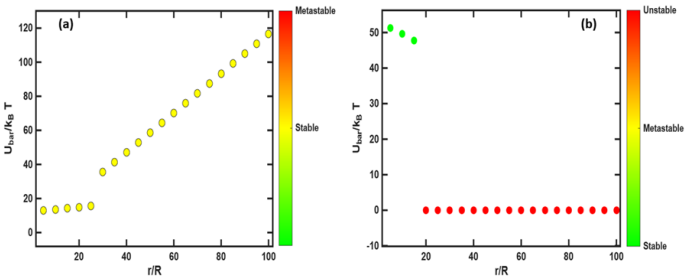

Figure 6 Classification of stability regime on the basis of energy barrier (a) Model-1 and (b) Model-2.

Model-2 shows a strong size-dependent transition to unstable regimes with increasing particle size. Only smaller particle sizes are classified into stable or metastable regimes with barrier height becoming zero for larger particles, which are then classified into the unstable regime. The corresponding size-dependent interaction energies, barrier heights, and forces for Model-2 are given in Table 10 (Supporting Information). These figures and tables together demonstrate the different stability regimes achieved for the two interaction models under the same electrostatic and hydrophobic conditions.

Table 10 Size-dependent interaction energies, forces, and stability regimes in Model-2 (h_f = 10%)

R (nm)	Primary min (k_BT)	Barrier (k_BT)	Stability Regime
5	-36.498	51.264	I
10	-22.998	49.57	I
15	-9.4983	47.792	I
20	0.84564	0	3
25	1.0571	0	3
30	1.2685	0	3
35	1.4799	0	3
40	1.6913	0	3
45	1.9027	0	3
50	2.1141	0	3
55	2.3255	0	3
60	2.5369	0	3
65	2.7483	0	3
70	2.9597	0	3
75	3.17121	0	3
80	3.3826	0	3
85	3.594	0	3
90	3.8054	0	3
95	4.0168	0	3
100	4.2282	0	3

Scaling behaviour and Debye length dependence

The size dependence of interparticle interactions was further analysed by studying the scaling behavior of the energy barrier and the maximum interaction force for both models under the same hydrophobic and electrostatic conditions. The interaction force was determined by taking the first derivative of the reduced interaction potential with respect to separation, and the maximum attractive force was obtained for each particle size. This approach provided a consistent measure of interaction strength across various sizes.

For Model-1, Figure 7(a) plots the energy barrier height and the maximum interaction force as functions of particle size. The corresponding data are summarized in Table 9 (Supporting Information). Moreover, Figure S3 plots the effect of electrostatic screening on the energy barrier, where the Debye length affects the size of the energy barrier but not its size dependence. The corresponding plot for Model-2 is shown in Figure 7(b). In this model, the energy barrier height goes to zero for small particle sizes, while the maximum interaction force depends systematically on particle size. The corresponding interaction energies, barrier heights, and forces are summarized in Table 10 (Supporting Information). Figure S3(b) shows that changes in Debye length will affect the magnitude of interaction force. But, it will not lead to the emergence of a finite barrier at large particle sizes.

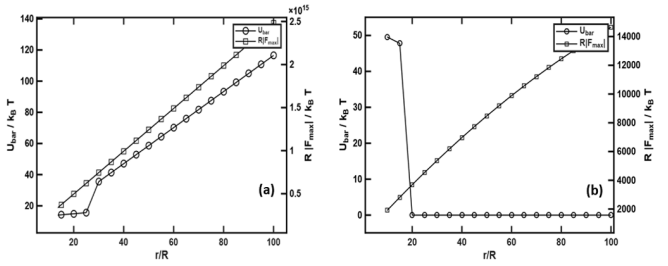

Figure 7 Dimensionless scaling of energy barrier and interaction force: (a) Model-1 and (b) Model-2.

Size effect on interaction forces

The plot of the maximum interaction force as a function of particle size highlights the characteristic scaling of the two models. In Model-1, the maximum interaction force is found to be linearly increasing with the particle size, as shown in Figure 8 (a). The corresponding linear fit has a high correlation coefficient, signifying a strong dependence on size of the particle and the interaction force magnitude.

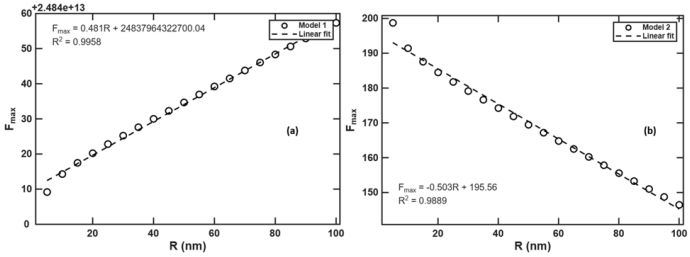

Figure 8 Maximum interaction force Fmax as a function of particle size R for Model-1 and Model-2 systems at a constant hydrophobic fraction, i.e., h_f = 10%. Notice the reversal of the slope on changing the non-DLVO component of the interaction. See text for details.

Citation: Neha VK, Bohidar HB. Aggregation of hydrophobic proteins: size dependent behavior and crossover to instability. *J Appl Biotechnol Bioeng* . 2026;13(3):91–98. DOI: 10.15406/jabb.2026.13.00422

By comparison, Model-2 exhibits a linear decrease in the maximum interaction force with increasing particle size, as shown in Figure 8 (b). Finite interaction forces are observed across the examined size range; however, no corresponding energy barrier is present

Discussions

Origin of kinetic stabilization in model-1

In Model-1, the interaction profile is characterized by the combined effect of short-range molecular attraction and electrostatic repulsion. While the Lennard-Jones interaction provides a strong short-range attraction which increases with particle size because of the larger effective interaction area, the double layer repulsion adds a stabilizing energy barrier at intermediate separations. As the particle size is increased, the strength of both the attractive and repulsive components grows, resulting in stronger interaction forces and higher barrier heights. Thus, while a strong primary minimum forms at short separations, the presence of a finite barrier prevents particles from easily accessing this configuration. Consequently, particles remain kinetically stabilized by the energy barrier, preventing spontaneous aggregation as shown in Figure 1.

Hydrophobicity driven destabilization and size crossover in Model-2

In Model-2, the interaction between particles varies significantly due to the presence of a short-range hydrophobic attraction represented by an exponential potential. For smaller particles, the hydrophobic attraction dominates the total interaction and results in a strong attractive well as the particles approach contact. Unlike molecular interactions, the hydrophobic contribution does not increase significantly with increasing particle size. As the particle size increases, electrostatic and surface interactions become stronger, and the hydrophobic attraction is no longer sufficient to maintain a stable interaction. This leads to a crossover behavior: smaller particles tend to bind together, whereas larger particles become unstable toward aggregation, as depicted in Figure 1.

Aggregation of elastin

Elastin is a hydrophobic fibrous protein found in the vertebrate tissues including major blood vessels, lungs, and skin. This biopolymer is associated with high shear elastic modulus that enables reversible stretching and recoiling. Such outstanding mechanical properties owe their origin to the regular arrangement of hydrophobic domains of non-polar amino acids like glycine, alanine, valine, and leucine and lysine in its molecular structure. Tropoelastin is the monomeric precursor for elastin, which is insoluble, non-glycosylated, and highly hydrophobic, and it undergoes self-aggregation, and phase separation following a complex thermodynamic process which is temperature dependent.[3,28] The aggregation behaviour of this physiologically important hydrophobic protein was extensively studied in ethanolic solvent by Pawar et al.[3] It was found that at above a threshold temperature ~ 297 K there was a propensity of hydrophobic interactions that caused enhanced protein aggregation. This was modeled via an extended-DLVO model by incorporating a surface tension force as the non-DLVO component in the constitutive equation (Eq.1). It was concluded that the hydrophobic interactions between the protein molecules were overwhelmingly dominant over other interactions which caused instability due to enhanced aggregation, which leads to liquid-liquid phase separation, often called coacervation.[28,29]

Let us apply the Model-2 interaction protocol to explain the aggregation behavior of elastin. This model stipulates that for small particles hydrophobic interaction dominates near contact, and unlike the molecular scale attraction this interaction doesn't change significantly with particle size until a limit. However, as size increases further electrostatic and contributions arising from surface-related forces become increasingly dominant, and the hydrophobic forces alone are inadequate to sustain a stabilizing barrier (primary minima). Consequently, a size-dependent crossover from attraction-dominated behavior at small size to an unstable interaction regime at larger size arises that may lead to a phase separation. In the elastin aggregation studies a similar growth of particle size dominated crossover from a stable one-phase dispersion (elastin solution) to a two-phase liquid-liquid phase separation was noticed, which was attributed to coacervation.[29] It is well known that coacervation is a thermodynamic phase transition triggered by strong associative interactions between polyelectrolytes.[30] Thus, we notice a qualitative concurrence of our model with the aggregation behavior reported for the hydrophobic protein elastin.

Aggregation of Zein

Zein is a class of prolamine protein (a group of plant proteins found with very high proline content) mostly found in maize. Zein is composed of large amount (> 50%) of hydrophobic amino acids, such as proline, glutamine, and asparagine, leucine and alanine, but low in the essential amino acids lysine and tryptophan. It is a storage protein and constitutes as much as half of the total protein of the endosperm. Zein has a helical wheel shaped structure with nine homologous units arranged in non-parallel with the units stabilized by hydrogen bonds. This helical shape gives zein a globular morphology. This water-insoluble, but alcohol-soluble corn storage protein is one of the poorly understood biomacromolecules as far as its aggregation properties under different solvent conditions are concerned.

It is reported that this hydrophobic plant protein forms nanoparticles in ethanolic solutions with specific aggregation attributes.[31] Homogeneous aggregates of low size and polydispersity were formed close to its pI (~6.2). In contrast, in the presence of a monovalent salt, these particles exhibited aggressive heterogeneous aggregation with the formation of large aggregates of high polydispersity.[31] Zein which contains large amounts of non-polar and hydrophobic amino acids aggregates readily following significantly different self-organization pathways in a dominant manifestation of interplay of various interactions in the milieu of a binary solvent. Here too, we may apply the implications of Model-2 to understand the aggregation kinetics of zein. It was noticed that maximum aggregation occurred at the isoelectric pH (pI) of zein which is 6.2. Thus, there was a propensity of aggregation when the net charge on the protein was marginal. In such a scenario the dominant contributions associative interactions would arise from the hydrophobic and surface forces. The particle size growth profile revealed a biphasic pattern with an initial sharp increase in aggregate size followed by a slower growth. In the absence of an electrical double layer, the hydrophobic attractive forces were dominant until a size of about two times the size of the original (monomer) was achieved. Beyond that there was a smooth cross-over led by surface forces that provoked aggregation albeit slowly, and large clusters emerged consistent with the predictions of Model-2.

Conclusions

This work investigates the phenomenon of protein aggregation via an extended version of the DLVO approach emphasizing hydrophobic interaction. A scaling relation was established between the interaction force and particle/biomolecular size which explicitly depends on the surface property. Model-1 focused on the attractive potential at the molecular-scale where the resulting interaction showed the presence of kinetically stabilized aggregation states. However, such models,

Citation: Neha VK, Bohidar HB. Aggregation of hydrophobic proteins: size dependent behavior and crossover to instability. *J Appl Biotechnol Bioeng* . 2026;13(3):91–98. DOI: 10.15406/jabb.2026.13.00422

which are suitable for conventional colloidal systems, may not always be realistic, especially considering the environment in which biomolecular systems resides. In contrast, Model 2, which emphasized the hydrophobic force showed barrier less interaction with deep primary minima. This result pertains to systems that follow diffusion-limited aggregation like hydrophobic proteins. Furthermore, it shows that smaller particles demonstrate DLVO-like behavior, whereas for systems with higher hydrophobic potentials form larger aggregates aggressively due to the absence of any energy barrier. Finally, it is necessary to comment on the experimental validation of the results obtained. Clearly, this requires hydrophobicity-dependent size data for proteins in a given system over a wide range, for which there is a paucity of data. Regardless, an attempt has been made to qualitatively discuss the aggregation behavior of two hydrophobic proteins, elastin and zein, within the ambit of one of the interaction models proposed in this work.

Acknowledgements

The research problem was conceptualized jointly by both authors, Neha performed the numerical analysis, results were discussed jointly, and the manuscript was written together. Both the authors consent to submit this work for publication.

Conflict of interest

Authors declare no conflict of interest.

References

1. Hummer G, Garde S, García AE, et al. Hydrophobic effects on a molecular scale. *J Phys Chem B*. 1998;102:10469–10482.
2. Bohidar HB, Fundamentals of polymer physics and molecular biophysics, Cambridge University Press, Cambridge, UK; 2015.
3. Pawar N, Kaushik P, Bohidar HB. Hydrophobic hydration and anomalous diffusion of elastin in an ethanolic solution. *Phys Chem Chem Phys*. 2017;19:13994–14000.
4. Lin YH, Song J, Forman-Kay JD, et al. Random-phase-approximation theory for sequence-dependent, biologically functional liquid-liquid phase separation of intrinsically disordered proteins. *J Mol Liq*. 2017;228:176–193.
5. Pulawski W, Ghoshdastider U, Andrisano V, et al. Ubiquitous amyloids. Appl Biochem Biotechnol. 2012;166:1626–1643.
6. Norris V, Oláh J, Krylov S, et al. The Sherpa hypothesis: Phenotype-protecting disordered proteins stabilize the phenotypes of neurons and oligodendrocytes. *Research Square*. 2023.
7. Stradner A, Schurtenberger P, Potential and limits of a colloid approach to protein solutions. *Soft Matter.* 2020;16:307–323.
8. Agmo Hernández V. An overview of surface forces and the DLVO theory. *ChemTexts*. 2023;9(10).
9. Horinek D. DLVO theory. In: Kreysa G, Ota K, Savinell RF, editors. Encyclopedia of Applied Electrochemistry, Springer, New York; 2014. p. 343–346.
10. Stoll S, Buffle J. Computer simulations of colloids and macromolecules aggregate formation: Kolumne; CHIMIA. 1995;49(300).
11. Mela I, Aumaitre E, Williamson AM, et al. Charge reversal by salt-induced aggregation in aqueous lactoferrin solutions. *Colloids Surf. B Biointerfaces*. 2010;78:53–60.
12. Li L, Zhang R, Guo Y, et al. Updated insights into the mechanism of salt-induced aggregation-based single-molecule surface-enhanced Raman spectroscopy. *Adv Sci*. 2025;12:2417025.
13. Pusara S, Yamin P, Wenzel W, et al. A coarse-grained xDLVO model for colloidal protein–protein interactions. *Phys Chem*. 2021;23:12780–12794.
14. Goswami S, Bajpai J, Bajpai AK. Designing gelatin nanocarriers as a swellable system for controlled release of insulin: An in-vitro kinetic study. *J Macromol Sci Part A*. 2019;47:119–130.
15. Cedano JA, Querol E, Mozo-Villarías A. How hydrophobicity shapes the architecture of protein assemblies. *Eur Phys E J*. 2023;46(7):62.
16. Schneider HJ. Distinction and quantification of noncovalent dispersive and hydrophobic effects. *Molecules*. 2024;29:1591.
17. Lim TC. The relationship between Lennard-Jones (12-6) and Morse potential functions. *Z Naturforsch A*. 2003;58:615–617.
18. Vijaykumar A, Ouldridge TE, ten Wolde PR, et al. Multiscale simulations of anisotropic particles combining molecular dynamics and Green's function reaction dynamics. *J Chem Phys*. 2017;146:114106.
19. Prausnitz JM. Molecular thermodynamics for some applications in biotechnology. *J Chem Thermodyn.* 2003;35:21–39.
20. Blanco MA, Sahin E, Robinson AS, et al. Coarse-grained model for colloidal protein interactions, B22, and protein cluster formation. *J Phys Chem B*. 2013;117:16013–16028.
21. Lower S. Hydrogen-bonding and water, Chem1 virtual textbook, Simon Fraser University.
22. Pellicane G, Costa D, Caccamo C. Theory and simulation of short-range models of globular protein solutions. *J Phys Condens Matter.* 2004;16:S4923–S4936.
23. Mani E, Lechner W, Kegel WK, et al. Equilibrium and non-equilibrium cluster phases in colloids with competing interactions. *Soft Matter*. 2014;10:4479–4486.
24. Bianco V, Franzese G. Hydrogen bond correlated percolation in a supercooled water monolayer as a hallmark of the critical region. *J Mol Liq*. 201;285:727–739.
25. Kirkwood JG. On the theory of strong electrolyte solutions. *J Chem Phys*. 1934;2:767–781.
26. Varilly P, Willard AP, Kirkegaard JB, et al. Intra-chain organisation of hydrophobic residues controls inter-chain aggregation rates of amphiphilic polymers. *J Chem Phys.* 2017;146:135102.
27. Auer S, Trovato A, Vendruscolo M. A condensation-ordering mechanism in nanoparticle-catalyzed peptide aggregation. *PLoS Comput Biol.* 2009;5:e1000458.
28. Muiznieks LD, Sharpe S, Pomès R, et al. Role of liquid–liquid phase separation in assembly of elastin and other extracellular matrix proteins. *J Mol Biol*. 2018430;23:4741–4753.
29. Kaushik P, Rawat K, Bohidar HB. Heat-induced coacervation of elastin and its possible thermoreversibility. *Colloid Polym Sci*. 2019;297:947–956.
30. Sing CE, Perry SL. Recent progress in the science of complex coacervation. *Soft Matter*. 2020;16:2885–2914.
31. Mallik A. A study on protein aggregation, M.Sc. thesis, School of Physical Science, Jawaharlal Nehru University, New Delhi, India; 2019.